

**Abundances in the H I envelope of the extremely low-metallicity Blue Compact Dwarf Galaxy SBS 0335–052 from *Far Ultraviolet Spectroscopic Explorer* observations**

Trinh X. Thuau

*Astronomy Department, University of Virginia, P.O. Box 3818, University Station,  
Charlottesville, VA, 22903*

[txt@virginia.edu](mailto:txt@virginia.edu)

Alain Lecavelier des Etangs

*Institut d’Astrophysique de Paris, CNRS, 98 bis Boulevard Arago, 75014 Paris, France*

[lecaveli@iap.fr](mailto:lecaveli@iap.fr)

and

Yuri I. Izotov

*Main Astronomical Observatory, National Academy of Sciences, 27 Zabolotnoho str., 03680 Kyiv,  
Ukraine*

[izotov@mao.kiev.ua](mailto:izotov@mao.kiev.ua)

## ABSTRACT

We present *FUSE* spectroscopy of SBS 0335–052, the second most metal-deficient blue compact dwarf (BCD) galaxy known ( $\log \text{O/H} = -4.70$ ). In addition to the H I Lyman series, we detect C II, N I, N II, O I, Si II, Ar I and Fe II absorption lines, mainly arising from the extended H I envelope in which SBS 0335–052 is embedded. No H<sub>2</sub> absorption lines are seen. The absence of diffuse H<sub>2</sub> implies that the warm H<sub>2</sub> detected through infrared emission must be very clumpy and associated with the star-forming regions. The clumps should be denser than  $\sim 1000 \text{ cm}^{-3}$  and hotter than  $\sim 1000 \text{ K}$  and account for  $\geq 5\%$  of the total H I mass. Although SBS 0335–052 is a probable young galaxy, its neutral gas is not pristine. The metallicity of its neutral gas is similar to that of its ionized gas and is equal  $\log \text{O/H} \sim -5$ . This metallicity is comparable to those found in the H I envelopes of four other BCDs with ionized gas metallicities spanning the wide range from  $\log \text{O/H} = -4.8$  to  $\log \text{O/H} = -3.8$ , and in Ly $\alpha$  absorbers, fueling the speculation that there may have been previous enrichment of the primordial neutral gas to a common metallicity level of  $\log \text{O/H} \sim -5$ , possibly by Population III stars.

---

Based on observations obtained with the NASA-CNES-CSA *Far Ultraviolet Spectroscopic Explorer*. *FUSE* is operated for NASA by the Johns Hopkins University under NASA contract NAS 5-32985.

*Subject headings:* galaxies: irregular — galaxies: abundances — galaxies: ISM — galaxies: individual (SBS 0335–052)

## 1. Introduction

The Blue Compact Dwarf (BCD) galaxy SBS 0335–052 (Izotov et al. 1990), with an ionized gas oxygen abundance of  $12 + \log \text{O/H} = 7.30$  (Melnick et al. 1992; Izotov et al. 1997, 1999) [ $Z_\odot/23$ , if the recent lower determination of the Oxygen abundance of the Sun  $12 + \log \text{O/H} = 8.66$  by Asplund et al. (2004) is adopted], is one of the most metal-deficient star-forming galaxies known, just after its dwarf irregular companion SBS 0335–052W ( $12 + \log \text{O/H} = 7.22$  or  $Z_\odot/28$ , Lipovetsky et al. 1999) and the BCD I Zw 18 ( $12 + \log \text{O/H} = 7.17$  or  $Z_\odot/31$ , Izotov et al. 1999). Because of its extremely low metallicity and its high neutral hydrogen content (Pustilnik et al. 2001), SBS 0335–052 is an excellent candidate for being a young galaxy, just like I Zw 18. The latter has been shown by Izotov & Thuan (2004) to be a bona fide young galaxy. Resolving I Zw 18 into stars with deep *Hubble Space Telescope* (*HST*)/Advanced Camera for Survey images and constructing its color-magnitude diagram (CMD), Izotov & Thuan (2004) have shown that the galaxy does not contain red giant stars and that the most evolved stars in it are not older than 500 Myr. Because of its larger distance (54.3 Mpc, Thuan et al. 1997, hereafter TIL97, instead of 15 Mpc for I Zw 18), SBS 0335–052 cannot be resolved into stars by *HST*, so its age cannot be determined directly by CMD analysis. However, using optical colors of the low surface brightness component together with evolutionary synthesis models, TIL97 and Papaderos et al. (1998) have constrained the age of the underlying stellar population to be less than  $\sim 100$  Myr. Near-infrared (NIR) colors after correction for gaseous emission are consistent with a stellar population not older than 4 Myr, with a possible contribution to the NIR light from an evolved stellar population not exceeding  $\sim 15\%$  (Vanzi et al. 2000). Östlin & Kunth (2001) have derived from surface photometry considerably larger ages for SBS 0335–052. However these large ages may be the consequence of their not subtracting out the large ionized gas contamination from the surface brightness profiles used. Recently, Pustilnik et al. (2004) have also found a young age for SBS 0335–052. Depending on the adopted star formation history of the BCD, they derive an age between 100 Myr and 400 Myr. In any case, SBS 0335–052 constitutes an excellent nearby laboratory for studying massive star formation and its interaction with the ambient interstellar medium (ISM) in a very metal-deficient environment. Most of the star formation in SBS 0335–052 occurs in six super-star clusters, roughly aligned in the southeast-northwest direction, with ages  $\leq 25$  Myr, within a region of  $\sim 2''$  or 520 pc in size (TIL97).

VLA observations have shown the presence of a massive ( $2.2 \times 10^9 M_\odot$ ) and extended (66 kpc  $\times$  22 kpc) neutral hydrogen gas envelope around SBS 0335–052 (Pustilnik et al. 2001). This H<sub>I</sub> envelope absorbs all the Ly $\alpha$  photons emitted by the young massive stars. Thuan & Izotov (1997) have obtained a *HST*/Goddard High Resolution Spectrograph (GHRS) spectrum of SBS 0335–052 which reveals a broad damped Ly $\alpha$  absorption with a high H<sub>I</sub> column density

$N(\text{H I}) = (7.0 \pm 0.5) \times 10^{21} \text{ cm}^{-2}$ , the largest known in a BCD. The *HST/GHRS* spectrum also shows absorption lines of several heavy elements such as O I, Si II and S II. Assuming that these absorption lines are not saturated, Thuan & Izotov (1997) found that the derived heavy element abundance in the neutral gas to be considerably lower than that of the ionized gas. Furthermore, Vanzi et al. (2000) have detected with infrared spectrophotometry molecular hydrogen in emission in SBS 0335–052. The presence of a neutral gas envelope around SBS 0335–052 and the detection of molecular hydrogen in emission make this galaxy an ideal target for *FUSE* spectroscopy. Using SBS 0335–052 as a source of UV light shining through the H I envelope, a *FUSE* absorption spectrum will allow us to determine independently the heavy element abundances in the neutral gas of the galaxy and check for the presence of H<sub>2</sub> in it.

We describe the *FUSE* observations in Section 2. In Section 3, we set upper limits on the amount of diffuse H<sub>2</sub>. In Section 4, we show that the warm H<sub>2</sub> detected through infrared emission must be very clumpy. We derive the column densities of the interstellar ionic species in the H I gas, and compare the heavy element abundances in the neutral and ionized gas in Section 5. We summarize our findings in Section 6.

## 2. Observations and data analysis

SBS 0335–052 has been observed with *FUSE* (Moos et al. 2000) through the  $30'' \times 30''$  LWRS large entrance aperture on 2001, September 26 for a total integration time of 24.4 ksec. The data have been processed with version 1.8.7 of the CALFUSE pipeline. The eight separate exposures have been aligned and coadded. This results in a set of four independent spectra, two spectra for the two long wavelength LiF channels covering the wavelength range  $\sim 1000\text{--}1187 \text{ \AA}$ , and two spectra for the two short wavelength SiC channels, covering the wavelength range  $\sim 900\text{--}1100 \text{ \AA}$ . After co-addition, the S/N ratio per resolution element and per channel is estimated to be about 2 below 1000  $\text{\AA}$  and about 4 above 1000  $\text{\AA}$ .

To derive the spectrum, special attention was paid to the background residual which is not negligible for this faint target. The background has been estimated both on spectra obtained off-target through other apertures and at the bottom of wide saturated lines. The background level is found to be between 0 and  $3 \times 10^{-15} \text{ erg cm}^{-2} \text{ s}^{-1} \text{ \AA}^{-1}$ . The line spread function has been estimated with the unresolved Galactic H<sub>2</sub> absorption lines. The resolution is found to be  $R = \Delta\lambda/\lambda \approx 12000$ .

The resulting spectrum of SBS 0335–052 shifted to its rest-frame is shown in Fig. 1. It exhibits two absorption-line systems at two different radial velocities. The first system at nearly zero radial velocity is attributed to the interstellar clouds in the Milky Way. The second system at  $\sim 4050 \text{ km s}^{-1}$  is attributed to the ISM in SBS 0335–052, as the H I velocity of the BCD is  $4057 \pm 5 \text{ km s}^{-1}$  (Pustilnik et al. 2001), in good agreement with the optical velocity obtained by Izotov et al. (1997). Absorption lines from the atomic and ionic species N I, P II, Fe II, and Ni II are observed in the Milky Way, while for SBS 0335–052, in addition to the H I Lyman series,

absorption lines from the atoms and ions C II, N I, N II, O I, Si II, Ar I, and Fe II are seen. In Fig. 1, the lines arising from SBS 0335–052 are labeled while those belonging to the Milky Way are indicated by tickmarks below the *FUSE* spectrum. For the characteristics of the electronic transitions of H<sub>2</sub>, we have used the wavelengths and oscillator strengths tabulated by Abgrall et al. (1993a,b) respectively for the Lyman and the Werner systems, and the inverses of the total radiative lifetimes tabulated by Abgrall et al. (2000). For atomic lines, we have used the data for resonance absorption lines tabulated by Morton (2003).

### 3. Upper limits on the diffuse H<sub>2</sub> content of SBS 0335–052

Molecular hydrogen is known to be present in SBS 0335–052 as Vanzi et al. (2000) have detected several H<sub>2</sub> emission lines in their low-resolution near-infrared spectrum of the star-forming region. These lines observed in the *K* band are generally consistent, within the errors, with both thermal and fluorescent excitation by the strong UV field. It is thus of great interest to check whether there are H<sub>2</sub> absorption lines in the *FUSE* spectrum of SBS 0335–052. We found no H<sub>2</sub> line at the radial velocity of the BCD (Fig. 1). We obtained the following 3  $\sigma$  upper limits for the H<sub>2</sub> column density:  $1.2 \times 10^{17}$  cm<sup>−2</sup>,  $1.4 \times 10^{17}$  cm<sup>−2</sup>,  $7.9 \times 10^{16}$  cm<sup>−2</sup>,  $3.4 \times 10^{17}$  cm<sup>−2</sup> and  $1.5 \times 10^{17}$  cm<sup>−2</sup> respectively for the J= 0, 1, 2, 3 and 4 levels. To set an upper limit on the total H<sub>2</sub> column density, we follow the procedure of Aloisi et al. (2003). We add the two upper limits for the J=0 and J=1 levels. For the higher J levels, we assume a temperature ( $T = 500$  K and  $T = 1000$  K), which determines the level populations, and then normalize the level populations so as to be consistent with the measured upper limits. We obtain upper limits for the total H<sub>2</sub> column density of  $3.7 \times 10^{17}$  cm<sup>−2</sup> for  $T = 500$  K and  $5.5 \times 10^{17}$  cm<sup>−2</sup> for  $T = 1000$  K. These upper limits for H<sub>2</sub> are more than two orders of magnitude larger than those established for the BCDs I Zw 18 (Aloisi et al. 2003; Lecavelier des Etangs et al. 2004) and Mrk 59 (Thuan et al. 2002) because of the larger distance of SBS 0335–052, its fainter apparent magnitude and its lower signal-to-noise ratio *FUSE* spectrum. They correspond to column densities above which the damping wings start to broaden appreciably the H<sub>2</sub> absorption lines. With a H I column density of  $7.0 \times 10^{21}$  cm<sup>−2</sup> as determined by the *HST/GHRS* damped Ly $\alpha$  profile (Thuan & Izotov 1997), this corresponds to a fraction of H<sub>2</sub> molecules  $f(\text{H}_2) = 1.1 \times 10^{-4}$  ( $T = 500$  K) and  $f(\text{H}_2) = 1.6 \times 10^{-4}$  ( $T = 1000$  K) where the fraction is defined as  $f(\text{H}_2) = 2n(\text{H}_2)/[2n(\text{H}_2)+n(\text{H I})]$ , and where  $n(\text{H}_2)$  and  $n(\text{H I})$  are the number densities of H<sub>2</sub> and H I.

Are the H<sub>2</sub> upper limits established by *FUSE* consistent with the expected fraction of H<sub>2</sub> molecules in SBS 0335–052? This fraction can be estimated in the following manner. As discussed by Vidal-Madjar et al. (2000), at equilibrium, when the formation of H<sub>2</sub> on dust equals its destruction rate by UV photons, then:

$$f(\text{H}_2) = 1.6 \times 10^{-34} \left( \frac{Z}{Z_{\odot}} \right) \left( \frac{F_{R_0}}{\text{erg s}^{-1} \text{cm}^{-2} \text{\AA}^{-1}} \right)^{-1} \left( \frac{R_0}{\text{kpc}} \right)^{-1} \left[ \frac{N(\text{HI})}{\text{cm}^{-2}} \right]. \quad (1)$$

Here  $F_{R_0}$  is the flux at 1000\AA of UV H<sub>2</sub> dissociating radiation at radius  $R_0$  from the central ionizing

clusters in SBS 0335–052,  $Z$  is the metallicity equal to  $Z_{\odot}/23$ , and  $N(\text{H I})$  is the H I column density. From the H I map of Pustilnik et al. (2001), we estimate  $R_0 = 10''$ , or 2.5 kpc for a H I column density level of  $7.2 \times 10^{20} \text{ cm}^{-2}$ . This corresponds to a H I number density  $n(\text{H I}) \sim 0.1 \text{ cm}^{-3}$ . Since the density of the H I is increasing inwards, we adopt for our calculations a mean value  $n(\text{H I}) = 1 \text{ cm}^{-3}$ .

The observed UV flux at  $1000\text{\AA}$  is  $1.7 \times 10^{-14} \text{ erg s}^{-1} \text{ cm}^{-2} \text{ \AA}^{-1}$  (Thuan & Izotov 1997). Correcting for interstellar extinction using  $A(1000\text{\AA}) = 5.742A_V$  (Cardelli et al. 1989) and  $A_V = 0.155 \text{ mag}$  (Schlegel et al. 1998), we obtain  $F_{cor} = 3.8 \times 10^{-14} \text{ erg s}^{-1} \text{ cm}^{-2} \text{ \AA}^{-1}$ . Then

$$F_{R_0} = F_{cor} \left( \frac{D}{R_0} \right)^2 = 1.7 \times 10^{-5} \text{ erg s}^{-1} \text{ cm}^{-2} \text{ \AA}^{-1}, \quad (2)$$

where  $D = 54.3 \text{ Mpc}$  is the distance of SBS 0335–052. Finally, from Eq. 1 we derive  $f(\text{H}_2) = 1.1 \times 10^{-10}$ , more than six orders of magnitude below and fully consistent with the upper limits derived from the *FUSE* spectrum.

#### 4. A clumpy interstellar medium

Is such a low fraction of H<sub>2</sub> consistent with the detection of near-infrared (NIR) H<sub>2</sub> emission lines in the star-forming region of SBS 0335–052 by Vanzi et al. (2000)? We note that such a question has also arisen in the context of a circumstellar disk observed by Lecavelier des Etangs et al. (2001) where H<sub>2</sub> is detected in the infrared, but where no UV absorption lines are seen. To address the question for SBS 0335–052, we have carried out calculations specifically for the H<sub>2</sub>(1,0)S(0) line with the wavelength of  $2.223 \mu\text{m}$ . The results for the other detected H<sub>2</sub> lines should not be too different. Vanzi et al. (2000) have obtained a flux of  $1.4 \times 10^{-16} \text{ erg s}^{-1} \text{ cm}^{-2}$  for the  $2.223 \mu\text{m}$  line in SBS 0335–052. Assuming that the NIR emission is the result of fluorescent excitation, the luminosity of the H<sub>2</sub>(1,0)S(0) line from the region with radius  $R_0$  is

$$L_{tot} = n(\text{HI})f(\text{H}_2)Qh\nu V, \quad (3)$$

where  $h\nu = 9 \times 10^{-13} \text{ erg}$  is the energy of the photon with wavelength  $2.223 \mu\text{m}$ , and  $V = 4\pi R_0^3/3 = 1.92 \times 10^{66} \text{ cm}^{-3}$  is the volume of the region with radius  $R_0$ . Following Black & Dalgarno (1976) and using the UV flux  $F_{R_0}$  given by Eq. 2, we calculate a cascade entry rate  $Q = 1.55 \times 10^{-11} \text{ cm}^{-3} \text{ s}^{-1}$ . We obtain from Eq. 3 the luminosity of the  $2.223 \mu\text{m}$  line to be  $L_{tot} = 1.82 \times 10^{33} \text{ erg s}^{-1}$ . The spectrum of Vanzi et al. (2000) was obtained through a  $1'' \times 1''$  aperture, which corresponds to a volume  $V_{\text{Vanzi}} = 1.38 \times 10^{64} \text{ cm}^{-3}$ . Thus,  $V_{\text{Vanzi}}/V = 7.2 \times 10^{-3}$  and we would predict  $L_{predicted} = 1.31 \times 10^{31} \text{ erg s}^{-1}$ , corresponding to a flux at Earth of  $2.4 \times 10^{-23} \text{ erg s}^{-1} \text{ cm}^{-2}$ . This is  $\sim 10^7$  times lower than the observed flux.

The large flux discrepancy comes very probably from our assumption that the interstellar medium of SBS 0335–052 is uniform. In all likelihood, the NIR H<sub>2</sub> emission comes, not from an

uniform low-density neutral medium, but from dense clumps. For such dense clumps, self-shielding of electronic transitions, which becomes important starting at  $N(\text{H}_2) \sim 10^{14} \text{ cm}^{-2}$  (Black & van Dishoeck 1987), further increases  $f(\text{H}_2)$ . Although the UV pumping decreases, thermal excitation of the  $\text{H}_2$  vibrational states becomes important since it scales as  $n(\text{H}) \times n(\text{H}_2)$ . Following Black & van Dishoeck (1987), we find that we can reproduce well the observed flux of the  $\text{H}_2(1,0)\text{S}(0)$   $2.223 \mu\text{m}$  line if it comes from an ensemble of clumps with a total mass  $\sim 10^8 M_\odot$ , or about 5% of the total  $\text{H I}$  mass in SBS 0335–052 of  $2.1 \times 10^9 M_\odot$  (Pustilnik et al. 2001), and if each clump has a number density  $n(\text{H I}) = 5 \times 10^3 \text{ cm}^{-3}$  and a temperature  $T = 10^3 \text{ K}$ . For such a clump to be stable against gravitational collapse, its mass has to be less than its Jeans mass which is  $\sim 5 \times 10^4 M_\odot$ . This means that there should be at least  $\sim 2000$  of these clumps. The fraction of  $\text{H}_2$  molecules in such clumps is  $f(\text{H}_2) = 5 \times 10^3 \times 6.8 \times 10^{-11} = 3.4 \times 10^{-7}$ . The total number of  $\text{H}_2$  molecules in such clumps is  $N_{\text{tot}} = f(\text{H}_2)M/m_{\text{H}} = 4.1 \times 10^{58}$ , where  $m_{\text{H}} = 1.673 \times 10^{-24} \text{ g}$  is the mass of the hydrogen atom. Then the luminosity emitted in the  $\text{H}_2(1,0)\text{S}(0)$  line is  $L = N_{\text{tot}}n(\text{H I})q\hbar\nu = 4.5 \times 10^{37} \text{ erg s}^{-1}$ , where  $q \sim 10^{-10} \exp(-6000/T) \text{ cm}^3 \text{s}^{-1}$  is the rate of collisional excitation. The flux at Earth is then  $1.4 \times 10^{-16} \text{ erg s}^{-1} \text{ cm}^{-2}$  in very good agreement with the observed flux for the  $\text{H}_2(1,0)\text{S}(0)$  line at  $2.223 \mu\text{m}$ . Because of the exponential temperature dependence of the rate of collisional excitation, the above estimate is very sensitive to the adopted temperature for the gaseous clumps. This temperature cannot be lower than  $\sim 1000 \text{ K}$ , since for lower temperatures, the total mass of the clumps needed to account for the observed  $\text{H}_2(1,0)\text{S}(0)$   $2.223 \mu\text{m}$  flux would exceed the  $\text{H I}$  mass of SBS 0335–052.

Our *FUSE* observations are not sensitive to such a clumpy  $\text{H}_2$  distribution. They can only probe diffuse  $\text{H}_2$  along the line of sights to the several thousands of UV-bright massive stars in SBS 0335–052. As in the cases of the BCDs I Zw 18 (Aloisi et al. 2003; Lecavelier des Etangs et al. 2004) and Mrk 59 (Thuan et al. 2002), the absence of diffuse  $\text{H}_2$  in SBS 0335–052 can be explained by the combined effects of a low  $\text{H I}$  density, a scarcity of dust grains on which  $\text{H}_2$  molecules can form, and a large UV flux which destroys molecules.

## 5. Heavy element abundances

### 5.1. Column densities

We now derive the column densities of the heavy elements in the neutral  $\text{H I}$  envelope of SBS 0335–052 by fitting the profiles of the metal absorption lines. Column densities have been calculated by profile fitting using the `Owens` procedure developed by Martin Lemoine and the *FUSE* French team. This code returns the most likely values of many free parameters like the Doppler widths and column densities through a  $\chi^2$  minimization of the difference between the observed and computed profiles. The latest version of this code is particularly suited to the characteristics of *FUSE* spectra. For example, it allows for a variation of the background level, for an adjustable line spread function as a function of the wavelength domain, and for shifts in wavelength scale. These

are taken as free parameters which depend on the wavelength region and are determined by a  $\chi^2$  minimization.

The derived column densities with their error bars are given in Table 1. We will be quoting  $1\sigma$  error bars throughout the paper. These have been estimated as usual by considering the  $\Delta\chi^2$  increase of the  $\chi^2$  of the fit (see Hébrard G., et al. 2002, for a full discussion of the fitting method and error estimation with the `Owens` code). These error bars include the uncertainties in the continuum, the intrinsic line widths ( $b$ ), the background residual and the instrumental line spread function. It is important to remark that the use of different lines with different oscillator strengths of the same species allows us to constrain reasonably well all these quantities. In particular, the line width is well constrained by strongly saturated lines. On the other hand, the instrumental line spread function is mainly constrained by the very narrow lines from H<sub>2</sub> in the Milky Way. The final results are obtained from a simultaneous self-consistent fit to all the data. In this final fit, the continuum, the background residual, the instrumental line spread function, and the physical parameters of the absorption lines are free parameters. They are estimated by determining the best  $\chi^2$  in the parameters' space.

For each wavelength domain, we use simultaneously the data from two different channels: the SiC 1 and SiC 2 channels for wavelengths between 940 and 990 Å, and the LiF 1 and LiF 2 channels for wavelengths above  $\sim 990$  Å (see Sahnow et al. 2000, for a description of the *FUSE* channels). Because of the low signal-to-noise ratio of the SBS 0335–052 *FUSE* spectrum, only lines that are more or less saturated are clearly detected. This explains the relatively large error bars on the estimated column densities. However, for most species detected in SBS 0335–052, we have for each species several absorption lines from different transitions with different oscillator strengths. This allows us to obtain reliable column densities despite the saturation of the lines. For example, several O I lines are detected. The O I column density is mainly constrained by the profiles of four strong transitions with rest wavelengths  $\lambda_0 = 929.5$  Å, 950.9 Å, 988.8 Å, and 1039.2 Å. For N I, we detect the well-known triplet at 1034–1035 Å. The ions N II and N II\* have transitions in the wavelength region around 1084–1085 Å which is usually unusable because of its location in the hole between the two LiF detectors (see e.g., Lecavelier des Etangs et al. 2004, in the case of I Zw 18). However, here the large redshift of SBS 0335–052 moves that region out of the hole and allows clear detections of these transitions in the LiF 1b and LiF 2a channels. Si II is detected only in the  $\lambda_0 = 1020.7$  Å transition, the line at  $\lambda_0 = 989.9$  Å being blended with a strong N III line. However with an optical depth of  $\sim 2$ , this line does not suffer from much saturation and allows a reliable column density determination, albeit with large error bars. On the other hand, C II which is also detected only in one transition at  $\lambda_0 = 1036.3$  Å, is strongly saturated. This makes its column density determination very sensitive to systematic errors and can explain its deviation from the abundance pattern found for other species (see Section 5.2).

With the exception of H I for which the strong damping wings in the Lyman  $\beta$  line allow a very accurate determination of the column density, Fe II is the species for which we have obtained the highest precision (Table 1). Fe II has indeed nine clearly detected lines at  $\lambda_0 = 1055$  Å, 1063 Å,

1064 Å, 1082 Å, 1097 Å, 1122 Å, 1125 Å, 1143 Å and 1145 Å. Those lines have optical depths ranging from  $\sim 2$  to  $\sim 30$ , which allows a good determination of the Fe II column density by co-adding the nine separate profiles to improve the signal-to-noise ratio. Fig. 2 shows the fit to the co-added continuum and Fe II line profile.

To better constrain the column densities, we have also used, in addition to the *FUSE* data, the low resolution *HST* spectra obtained with the GHRS spectrograph and the G160M and G140L gratings by Thuan & Izotov (1997). These spectra show absorption lines of C II (1334.5 Å), O I (1302.2 Å) and Si II (1190.4, 1193.3, 1260.4 and 1304.4 Å).

For the species which are detected in both *FUSE* and *HST* spectra (O I, C II and Si II), the column densities given in Table 1 are derived from a simultaneous fit of both spectra. This assumes that both instruments cover the same spatial regions in the BCD, although the observations have been obtained through very different aperture sizes, 30'' in the case of *FUSE*, and 2'' for *HST*. This assumption is reasonable as the brightest star-forming clusters in SBS 0335–052 are confined within a very compact region ( $\lesssim 2''$ , TIL97), and this region is fully sampled by both *FUSE* and *HST* apertures. That this is indeed the case is confirmed by the fact that the H I column densities derived independently from the *FUSE* and *HST* spectra are very similar: the *FUSE* column density is  $\log N(\text{H I}) = 21.86^{+0.08}_{-0.05}$ , while the *HST* column density is  $\log N(\text{H I}) = 21.85 \pm 0.05$ . The heavy element column densities derived from the *FUSE* spectra alone and from the *FUSE+HST* spectra are consistent with each other within the errors. But by using the *FUSE* and *HST* spectra together, we are able to decrease the error bars by a factor of about 2. For example, the derived column density of C II using only the *FUSE* spectrum is  $\log N(\text{C II})$  (*FUSE*) =  $17.68^{+0.23}_{-1.6}$  as compared to  $\log N(\text{C II})$  (*HST+Fuse*) =  $17.59^{+0.23}_{-0.65}$ .

The simultaneous fit of a large set of lines with different oscillator strengths for the same species, and of many different species with the same intrinsic line width allows us to constrain the line broadening parameter (or Doppler width)  $b$ . In other words, a single  $b$  value is derived which gives the best simultaneous fit to the profile of every detected line of each species. As an example, Fig. 3 shows the fit to the O I  $\lambda 1039$  line. From the *FUSE* spectrum alone, we obtain  $b = 12.0^{+2.0}_{-1.2}$  km s $^{-1}$ . The error bar on the  $b$  value includes the uncertainties in the continuum level, the background residual, the instrumental line spread function and the column densities of the different species detected at the redshift of SBS 0335–052. If the *FUSE* and *HST* spectra are taken together, we obtain  $b = 11.3^{+1.4}_{-1.2}$  km s $^{-1}$ . The two  $b$  values are in good agreement and thus  $b$  is well constrained.

A  $b$  value of 12 km s $^{-1}$  would correspond to a velocity dispersion  $\sigma$  of only  $b/\sqrt{2} = 8.5$  km s $^{-1}$ , somewhat smaller than the value of  $\sim 15$  km s $^{-1}$  derived from the H I VLA map of SBS 0335–052 (Pustilnik et al. 2001), although the two values are not directly comparable: the radio observations measure the velocity dispersion within a region equal to the VLA beam size of 20''.5  $\times$  15''.0, while the *FUSE* observations probe only the star-forming region of  $\sim 2''$  in size. Note that if  $b$  is underestimated, the column densities derived from very saturated lines would be overestimated.

For instance, we estimate that if the real value of the  $b$  parameter is  $16 \text{ km s}^{-1}$ , the column density of O I would be overestimated by  $\sim 1$  dex. As for C II, the species for which the column density estimate is most sensitive to the  $b$  value, it would be overestimated by  $\sim 1.3$  dex. Other species are less sensitive to the exact value of  $b$ , making the determination of their column densities more robust.

## 5.2. Modeling

We use the CLOUDY code (Ferland 1996; Ferland et al. 1998, version c90.05) to construct a photoionized H II region model that best reproduces the optical nebular emission-line intensities observed in SBS 0335–052 (Izotov et al. 1997). By comparing the H II column densities predicted by CLOUDY with the (H I + H II) column densities observed by *FUSE*, we will be able to deduce the relative amounts of heavy elements in the H I and H II gas.

We consider a spherically symmetric ionization-bounded H II region model. The calculations are stopped in the zone away from the ionizing stars where the temperature drops to 2000 K. The ionization in this zone is very low and it is taken to be the outer edge of the H II region. Several input parameters need to be set. For a distance of 54.3 Mpc and using the aperture-corrected H $\beta$  flux from Izotov et al. (1997), we set the H $\beta$  luminosity to be  $L(\text{H}\beta) = 7.9 \times 10^{40} \text{ erg s}^{-1}$ , and the number of ionizing photons to be  $N(\text{Lyc}) = 1.7 \times 10^{53} \text{ s}^{-1}$ . We use the Kurucz (1991) stellar atmosphere models and adopt the effective temperature of the ionizing stellar radiation to be  $T_{\text{eff}} = 50000 \text{ K}$ , a typical value for low-metallicity high-excitation H II regions. For the inner radius of the H II region, we adopt  $R_{\text{in}} = 1.0 \times 10^{19} \text{ cm}$ . The chemical composition of the H II region is set by the observed element abundances derived from optical spectroscopy of SBS 0335–052 (Izotov et al. 1997), except for the carbon, silicon and phosphorus abundances. For carbon we adopt  $\log \text{C/O} = -0.83$ , and for silicon  $\log \text{Si/O} = -1.60$  (Izotov & Thuan 1999). As for phosphorus, we adopt the solar  $\log \text{P/O} = -3.42$  of Grevesse & Noels (1996). The adopted abundances are shown in Table 2.

We run the CLOUDY code varying the filling factor  $f$  and the electron number density  $N_{\text{e}}$  in order to obtain the best agreement between the predicted and observed [O II] and [O III] emission lines. We find that if  $N_{\text{e}}$  varies in the ranges  $7 - 13 \text{ cm}^{-3}$  and  $f$  in the range  $0.17 - 0.29$ , then we have adequate agreement between the observed and model line intensities. The best model is found for a filling factor  $f = 0.22$  and an electron number density  $N_{\text{e}} = 10 \text{ cm}^{-3}$ . The optical line intensities of the best model are shown in Table 3, where we compare them with the observed ones (Izotov et al. 1997). The error bars of the model line intensities (and those of the model parameters in Tables 1 and 4) correspond to the maximum range of their values. There is good general agreement between observed and model line intensities, giving us confidence that the photoionization model is correct. The predicted total hydrogen (neutral and ionized) column density in the H II region is  $N(\text{H I} + \text{H II}) = 4.93 \times 10^{21} \text{ cm}^{-2}$  or  $\log N(\text{H I} + \text{H II}) = 21.69$ . As expected for a H II region model, most of the hydrogen is ionized:  $N(\text{H II}) = 4.89 \times 10^{21} \text{ cm}^{-2}$ . The column density of the

neutral hydrogen is two orders of magnitude lower. The model also predicts a column density of molecular hydrogen made via  $H^- N(H_2) = 1.91 \times 10^{11} \text{ cm}^{-2}$ , more than six orders of magnitude lower than our observational upper limit.

We now compare the column densities of heavy elements predicted by CLOUDY with those derived from the *FUSE* and *HST* spectra. The CLOUDY predicted column densities are given in Table 4. Those relevant to the *FUSE* observations are also repeated in column 3 of Table 1. In Table 4,  $x$  is the radially averaged ratio of the ion number to the total number of a particular element, e.g.,  $N(Fe^+)/N(Fe)$ . The predicted  $\log N(X)$  of species X is then derived as  $\log N(X) = \log N(H\,I+H\,II) + \log X^{+i}/H - \log x(X^{+i})$ . The column densities listed in Table 1 are plotted with their  $1\,\sigma$  error bars as filled circles in Fig. 4. For comparison, the corresponding CLOUDY predicted column densities are plotted as open circles. There are two features that should be noted. First, the observed and calculated relative variations from ionic element to ionic element show the same pattern. While this simply reflects the relative cosmic abundances of the considered species, retrieving that pattern from the data does show the consistency of the derived column densities for different species despite the low signal-to-noise ratio of our *FUSE* spectra.

Second, the majority of the calculated  $H\,II$  column densities are systematically smaller by more than one order of magnitude than the observed column densities. This implies that the *FUSE* column densities arise mainly in the  $H\,I$  neutral envelope, and not in the gas ionized by young stars.

Fig. 5 shows the ratio of the column densities of all ions relative to that of  $O\,I$ . As for the column density of  $O\,I$ , it is given relative to that of  $H\,I$ . There is general good agreement between the ratios of the *FUSE* column densities (filled circles) and the ratios of the elements abundances in the  $H\,II$  region (stars). The only exception is the  $N(C\,II)/N(O\,I)$  ratio which is a factor of 30 larger than the  $C/O$  ratio in the  $H\,II$  region. As discussed in Section 5.1, the  $C\,II$  column density is derived from a single strongly saturated line and is probably overestimated.

Of special interest is the  $N(O\,I)/N(H\,I)$  ratio. The ionization potential of  $O\,I$  is very similar to that of  $H\,I$ , and there is an efficient charge exchange between  $O\,II$  and  $H\,I$ . Hence there is a strong coupling between the oxygen and hydrogen ionization fractions. In the neutral gas, the  $O\,I/H\,I$  ratio can therefore be considered as a very good proxy for the  $O/H$  ratio and hence it is a very good tracer of metallicity. We obtain  $\log N(O\,I)/N(H\,I) = -5.04 \pm 0.55$  or  $[O\,I/H\,I] = -1.70$ . This is to be compared with  $\log O/H = -4.70 \pm 0.01$  for the ionized gas in SBS 0335–052 (Izotov et al. 1999). Thus, within the errors, the metallicity of the neutral gas in SBS 0335–052 is comparable to that of its ionized gas. The much lower metallicity of the neutral gas of SBS 0335–052 obtained by Thuan & Izotov (1997) from *HST* observations is not correct as it is based on the erroneous assumption that the  $O\,I$ ,  $Si\,II$  and  $S\,II$  lines are not saturated.

How does the metallicity of the  $H\,I$  gas in SBS 0335–052 compare with those determined in the neutral ISM of other BCDs? Such a determination has been made for four other BCDs. For the most metal-deficient BCD known, I Zw 18 with a  $\log (O/H)_i$  of the ionized gas equal to –

$4.82 \pm 0.01$  (Izotov & Thuan 1999), Aloisi et al. (2003) have obtained  $\log(O/H)_n$  of the neutral gas  $= -5.37 \pm 0.28$  while Lecavelier des Etangs et al. (2004) derived the higher value  $\log(O/H)_n = -4.7 \pm 0.35$ . The discrepancy between the two values may be due to the fact that, to derive O/H, Aloisi et al. (2003) use the strongly saturated O I line at  $\lambda_0 = 1039$  Å which, at the redshift of I Zw 18, is blended with terrestrial airglow. For I Zw 36  $\equiv$  Mrk 209 with  $\log(O/H)_i = -4.23 \pm 0.01$  (Izotov & Thuan 1999), Lebouteiller et al. (2004) derived  $\log(O/H)_n = -4.5^{+1.0}_{-0.6}$ . For the BCD Mrk 59 with  $\log(O/H)_i = -4.01 \pm 0.01$  (Izotov & Thuan 1999), Thuan et al. (2002) have derived  $\log(O/H)_n = -5.0 \pm 0.3$ . As for the BCD NGC 1705 with  $\log(O/H)_i = -3.79 \pm 0.05$  (Lee & Skillman 2004), Heckman et al. (2001) have derived  $\log(O/H)_n = -4.6 \pm 0.3$ . Thus if we disregard the low value of Aloisi et al. (2003), the ionized gas metallicity of the five different BCDs observed by *FUSE* span a  $\log(O/H)_i$  range from  $-4.82$  to  $-3.79$ , i.e. a 1.03 dex spread. On the other hand, the metal content in their H I envelopes varies in the range  $\log(O/H)_n = -5.0$  -  $-4.5$ , or  $[O/H]_n = -1.7$  -  $-1.2$ , using the revised solar abundance  $(O/H)_\odot = -3.34$  of Asplund et al. (2004), i.e. a 0.5 dex spread.

At first glance, the metallicity spread of the neutral gas component appears to be only slightly lower than that of the ionized gas component. However a real difference appears once the error bars of the metallicity measurements are considered. The metallicities of the ionized gas,  $\log(O/H)_i$ , are determined from emission-line spectra with a precision of 0.01 dex (0.05 dex for NGC 1705), while those of the neutral gas,  $\log(O/H)_n$ , derived from absorption spectra, have considerably larger error bars varying from 0.3 dex for Mrk 59 and NGC 1705 to 1.0 dex for I Zw 36. These large error bars are in fact responsible for the apparent large metallicity spread of the neutral gas. If we take into account the error bars, the  $\log(O/H)_i$  values do vary over a 1.0 dex range while the  $\log(O/H)_n$  measurements are consistent with a single constant value. The spread of the  $\log(O/H)_n$  measurements around their mean value  $\langle \log(O/H)_n \rangle = -4.8$  can be evaluated by the sum of their squared normalized differences which, for five measurements, follow a  $\chi^2_4$  law with four degrees of freedom. We obtain a very low dispersion  $\sum [(\log(O/H)_n - \langle \log(O/H)_n \rangle)/\sigma]^2 = 1.40$ . There is more than 84% chance that  $\chi^2_4$  is larger than this value, supporting our contention that all five measurements are consistent with a single value of  $\log(O/H)_n$ .

The fact that the most metal-deficient BCD (I Zw 18) has about the same  $\log(O/H)_n$  as the most metal-rich BCD (NGC 1705) studied thus far by *FUSE* suggests that the metallicities of the neutral and ionized gas are unrelated. As discussed in the Introduction, the two most metal-deficient BCDs known, I Zw 18 and SBS 0335-052 have been suggested to be bona fide young galaxies, with an age not exceeding 500 Myr [see Izotov & Thuan (2004) for a discussion of the age of I Zw 18 and TIL97, Papaderos et al. (1998) and Pustilnik et al. (2004) for a discussion of the age of SBS 0335-052]. Thus the H I envelopes that surround these two BCDs may be expected to be truly primordial, i.e. not to contain heavy elements. Our study here of SBS 0335-052 and previous work on I Zw 18 show that this is clearly not the case, that the H I envelopes in these two BCDs have been enriched previously to a level  $[O/H]_n = -1.7$  -  $-1.4$ , perhaps by Population III stars. This speculation appears to be supported by the oxygen abundances derived by Telfer

et al. (2002) for the intergalactic medium using ultraviolet absorption lines in Ly $\alpha$  absorbers. Those authors derive a [O/H] range of  $-2.0$  to  $-1.1$  [we have corrected their values using the O solar abundance of Asplund et al. (2004)], which overlaps well with that derived thus far for the neutral ISM in five BCDs.

## 6. Conclusions

We present *FUSE* far-UV spectra of the second most metal-deficient Blue Compact Dwarf (BCD) galaxy known, SBS 0335–052 with an ionized gas oxygen abundance  $\log \text{O/H} = -4.70 \pm 0.01$ . Because this galaxy is one of the best candidates for being a young galaxy in the local universe, with an age not exceeding  $\sim 100$  Myr, the study of the abundances in its neutral hydrogen envelope is of special interest as it can shed light on the possible metal enrichment of the intergalactic medium by Population III stars several hundred million years after the Big Bang. We have obtained the following results:

1. No H<sub>2</sub> absorption lines are detected. We set a  $3\sigma$  upper limit for diffuse H<sub>2</sub> in SBS 0335–052 of  $3.7 \times 10^{17} \text{ cm}^{-2}$  for  $T = 500 \text{ K}$  and  $5.5 \times 10^{17} \text{ cm}^{-2}$  for  $T = 1000 \text{ K}$ . The absence of diffuse H<sub>2</sub> is due to the combined effects of a low H I density, a large UV flux which destroys H<sub>2</sub> molecules and a low metallicity which makes grains on which to form H<sub>2</sub> molecules scarce.
2. The non-detection of diffuse H<sub>2</sub> contrasts with the detection of H<sub>2</sub> emission lines in near-infrared spectra of SBS 0335–052. This implies that the detected H<sub>2</sub> must be clumpy, and associated only with the dense star-forming regions. These clumps should be denser than  $\sim 1000 \text{ cm}^{-3}$  and have a temperature greater than  $\sim 1000 \text{ K}$ . For such dense clumps, H<sub>2</sub> self-shielding can protect the H<sub>2</sub> molecules from dissociating UV-photons. Each clump has a mass less than  $\sim 5 \times 10^4 M_\odot$ . There should be at least  $\sim 2000$  clumps, accounting for  $\geq 5\%$  of the total H I mass.
3. The O I/H I ratio in the H I gas ( $\log N(\text{O I})/N(\text{H I}) = -5.04 \pm 0.55$ ) is similar, within the errors, to the O/H ratio derived from optical emission lines in the H II region of SBS 0335–052 ( $\log \text{O/H} = -4.70 \pm 0.01$ ), i.e. the metallicity of the neutral gas is comparable to that of the ionized gas. Thus although SBS 0335–052 is a probable young galaxy, its neutral envelope is not pristine.
4. There exists a noteworthy similarity between the O/H ratio observed in the H I gas of SBS 0335–052 (with  $\log (\text{O/H})_i$  of the ionized gas equal to  $-4.70$ ) and the ones seen in the H I gas of other BCDs for which similar *FUSE* studies have been carried out, I Zw 18 [ $\log (\text{O/H})_i = -4.82$ ], I Zw 36 [ $\log (\text{O/H})_i = -4.23$ ], Mrk 59 [ $\log (\text{O/H})_i = -4.01$ ] and NGC 1705 [ $\log (\text{O/H})_i = -3.79$ ]. In all five BCDs,  $\log \text{O/H}$  of the neutral gas is in the range  $-5.0$  -  $-4.5$  (or  $[\text{O/H}] = -1.7$  -  $-1.2$ ), although the ionized gas of NGC 1705 is some 10 times more metal-rich than that of SBS 0335–052 and I Zw 18. This suggests that the metallicities of the neutral and ionized gas components are unrelated. We may speculate that the neutral gas in these five BCDs has been enriched to a common metallicity level of  $\log (\text{O/H}) \sim -5$  by population III stars. This speculation appears to be supported by observations of Ly $\alpha$  absorbers which give similar oxygen abundances

in the intergalactic medium.

T.X.T. thanks the hospitality of the Institut d'Astrophysique de Paris. A.L. and Y.I.I. acknowledge the hospitality of the Astronomy Department of the University of Virginia. T.X.T. has been supported in part by NASA grant NAG5-10341. T.X.T and Y.I.I. are grateful for the partial financial support of the U.S. Civilian Research & Development Foundation for the Independent States of the Former Soviet Union (CRDF) through Award No. UP1-2551-KV-03, and of the National Science Foundation through grant AST-02-05785. This work has been done using the profile fitting procedure `Owens.f` developed by M. Lemoine and the *FUSE* French Team.

## REFERENCES

Abgrall, H., Roueff, E., Launay, F., Roncin, J. Y., & Subtil, J. L. 1993a, A&AS, 101, 273  
———. 1993b, A&AS, 101, 323

Abgrall, H., Roueff, E., & Drira, I. 2000, A&AS, 141, 297

Aloisi, A., Savaglio, S., Heckman, T. M., Hoopes, C. G., Leitherer, C., & Sembach, K. R. 2003, ApJ, 595, 760

Asplund, M., Grevesse, N., Sauval, A.J., Allende Prieto, C., & Kiselman, D. 2004, A&A, 417, 751

Black, J. H., & Dalgarno, A. 1976, ApJ, 203, 132

Black, J. H., & van Dishoeck, E. F. 1987, ApJ, 322, 412

Cardelli, J. A., Clayton, G. C., & Mathis, J. S. 1989, ApJ, 345, 245

Ferland, G. J. 1996, CLOUDY (Univ. of Kentucky Dept. of Phys. and Astron. Internal Rep.)

Ferland, G. J., Korista, K. T., Verner, D. A., Ferguson, J. W., Kingdon, J. B., & Verner, E. M. 1998, PASP, 110, 761

Grevesse, N., & Noels, A. 1996, in Cosmic Abundances, ed. S. S. Holt & G. Sonneborn (ASP Conference Series, 99), 117

Hébrard, G., Lemoine, M., Vidal-Madjar, A., et al. 2002, ApJS, 140, 103

Heckman, T.M., Sembach, K.R., Meurer, G.R., Strickland, D.K., Martin, C.L., Calzetti, D., & Leitherer, C. 2001, ApJ, 554, 1021

Izotov, Y. I., & Thuan, T. X. 1999, ApJ, 511, 639  
———. 2004, ApJ, December 1

Izotov, Y. I., Lipovetsky, V. A., Guseva, N. G., Kniazev, A. Y., & Stepanian, J. A. 1990, *Nature*, 343, 238

Izotov, Y. I., Lipovetsky, V. A., Chaffee, F. H., Foltz, C. B., Guseva, N. G., & Kniazev, A. Y. 1997, *ApJ*, 476, 698

Izotov, Y. I., Chaffee, F. H., Foltz, C. B., et al. 1999, *ApJ*, 527, 757

Kurucz, R. L. 1991, in *Stellar Atmospheres: Beyond Classical Models*, ed. L. Crivellari, I. Hubeny & D. G. Hummer (NATO ASI ser. C, 341; Dordrecht: Kluwer), 441

Lebouteiller, V., Kunth, D., Lequeux, J., Lecavelier des Etangs, A., Désert, J.-M., Hébrard, G. 2004, *A&A*, 415, 55

Lecavelier des Etangs, A., Vidal-Madjar, A., Roberge, A., et al. 2001, *Nature*, 412, 706

Lecavelier des Etangs, A., Désert, J.-M., Kunth, D., Vidal-Madjar, A., Callejo, G., Ferlet, R., Hébrard, G., & Lebouteiller, V. 2004, *A&A*, 413, 131

Lee, H., & Skillman, E. D. 2004, *ApJ*, 614, 698

Lipovetsky, V. A., Chaffee, F. H., Izotov, Y. I., Foltz, C. B., Kniazev, A. Y., & Hopp, U. 1999, *ApJ*, 519, 177

Melnick, J., Heydari-Malayeri, M., & Leisy, P. 1992, *A&A*, 253, 16

Moos, H. W., Cash, W. C., Cowie, L. L., et al. 2000, *ApJ*, 538, L1

Morton, D. C. 2003, *ApJS*, 151, 403

Östlin, G., & Kunth, D. 2001, *A&A*, 371, 429

Papaderos, P., Izotov, Y. I., Fricke, K. J., Guseva, N. G., & Thuan, T. X. 1998, *A&A*, 338, 43

Pustilnik, S. A., Brinks, E., Thuan, T. X., Lipovetsky, V. A., & Izotov, Y. I. 2001, *AJ*, 121, 1413

Pustilnik, S. A., Pramskij, A. G., & Kniazev, A. Y. 2004, *A&A*, 425, 51

Schlegel, D. J., Finkbeiner, D. P., & Davis, M. 1998, *ApJ*, 500, 525

Sahnow, D. J., Moos, H. W., Ake, T. B., et al. 2000, *ApJ*, 538, L7

Telfer, R. C., Kriss, G. A., Zheng, W., Davidsen, A. F., & Tytler, D. 2002, *ApJ*, 579, 500

Thuan, T. X., & Izotov, Y. I. 1997, *ApJ*, 489, 623

Thuan, T. X., Izotov, Y. I., & Lipovetsky, V. A. 1997, *ApJ*, 477, 661 (TIL97)

Thuan, T. X., Lecavelier des Etangs, A., & Izotov, Y. I. 2002, *ApJ*, 565, 941

Vanzi, L., Hunt, L. K., Thuan, T. X., & Izotov, Y. I. 2000, A&A, 363, 493  
Vidal-Madjar, A., Kunth, D., Lecavelier des Etangs, A., et al. 2000, ApJ, 538, L77

Table 1. Heavy element column densities ( $\text{cm}^{-2}$ ) in SBS 0335–052

Species	$\log N$ ( $\text{cm}^{-2}$ ) <sup>a</sup>	CLOUDY <sup>b</sup>
H I ( <i>FUSE</i> )	$21.86^{+0.08}_{-0.05}$	$21.69^{+0.12}_{-0.11}$
C II	$17.59^{+0.23}_{-0.65}$	$14.55^{+0.02}_{-0.02}$
N I	$14.84^{+0.25}_{-0.2}$	$13.13^{+0.01}_{-0.00}$
N II	$15.35^{+1.0}_{-0.75}$	$13.73^{+0.02}_{-0.01}$
N II*	$13.70^{+0.25}_{-13.70}$	
N III	$18.70^{+1.0}_{-18.7}$	$15.29^{+0.10}_{-0.10}$
O I	$16.82^{+0.5}_{-0.6}$	$14.86^{+0.01}_{-0.01}$
Si II	$14.90^{+0.45}_{-0.35}$	$13.96^{+0.04}_{-0.04}$
Ar I	$13.85^{+0.3}_{-0.55}$	$12.32^{+0.01}_{-0.01}$
P II	$14.00^{+1.0}_{-1.5}$	$12.06^{+0.01}_{-0.01}$
P II*	$13.09^{+0.5}_{-13.}$	
Fe II	$15.44^{+0.1}_{-0.15}$	$13.60^{+0.02}_{-0.01}$

<sup>a</sup>Fitting with a single Voigt profile. Error bars are  $1\sigma$  limits.

<sup>b</sup>Total H I + H II column density in the H II region.

Table 2. Abundances in SBS 0335–052 used as input to CLOUDY

Species	$\log (N(\text{species})/N(\text{H}))$
He	–1.0915 <sup>a</sup>
C	–5.50 <sup>b</sup>
N	–6.26 <sup>a</sup>
O	–4.67 <sup>a</sup>
Ne	–5.48 <sup>a</sup>
Si	–6.27 <sup>b</sup>
P	–8.05 <sup>c</sup>
S	–6.23 <sup>a</sup>
Ar	–6.93 <sup>a</sup>
Fe	–6.10 <sup>a</sup>

<sup>a</sup>From Izotov et al. (1997).

<sup>b</sup>From Izotov & Thuau (1999).

<sup>c</sup>Adopting solar  $\log \text{P}/\text{O} = -3.42$   
from Grevesse & Noels (1996).

Table 3. Comparison between the observed and CLOUDY predicted optical line intensities normalized to  $H\beta$

Ion	Observed <sup>a</sup>	CLOUDY
3727 [O II]	0.233	$0.217^{+0.046}_{-0.041}$
3835 H9	0.079	$0.079^{+0.000}_{-0.000}$
3868 [Ne III]	0.239	$0.253^{+0.014}_{-0.014}$
3889 He I + H8	0.172	$0.194^{+0.002}_{-0.001}$
3968 [Ne III] + H7	0.239	$0.239^{+0.004}_{-0.003}$
4101 H $\delta$	0.255	$0.264^{+0.000}_{-0.000}$
4340 H $\gamma$	0.476	$0.474^{+0.001}_{-0.000}$
4363 [O III]	0.109	$0.102^{+0.008}_{-0.009}$
4471 He I	0.035	$0.035^{+0.001}_{-0.000}$
4658 [Fe III]	0.003	$0.002^{+0.001}_{-0.000}$
4740 [Ar IV]	0.009	$0.007^{+0.001}_{-0.001}$
4861 H $\beta$	1.000	$1.000^{+0.000}_{-0.000}$
4959 [O III]	1.054	$1.099^{+0.061}_{-0.060}$
5007 [O III]	3.155	$3.173^{+0.172}_{-0.175}$
5876 He I	0.100	$0.095^{+0.000}_{-0.000}$
6300 [O I]	0.007	$0.002^{+0.000}_{-0.001}$
6312 [S III]	0.006	$0.013^{+0.000}_{-0.001}$
6563 H $\alpha$	2.745	$2.840^{+0.007}_{-0.008}$
6584 [N II]	0.007	$0.004^{+0.001}_{-0.000}$
6678 He I	0.027	$0.027^{+0.000}_{-0.000}$
6717 [S II]	0.019	$0.013^{+0.002}_{-0.003}$
6731 [S II]	0.017	$0.009^{+0.002}_{-0.001}$
7065 He I	0.039	$0.024^{+0.001}_{-0.001}$
7136 [Ar III]	0.014	$0.029^{+0.001}_{-0.001}$

<sup>a</sup>From Izotov et al. (1997).

Table 4. CLOUDY predicted column densities in the H II region

Ion	$\log x^a$	$\log N^b$
C II	$-1.640^{+0.091}_{-0.093}$	$14.55^{+0.02}_{-0.02}$
N I	$-2.295^{+0.108}_{-0.114}$	$13.13^{+0.01}_{-0.00}$
N II	$-1.700^{+0.096}_{-0.102}$	$13.73^{+0.02}_{-0.01}$
N III	$-0.141^{+0.011}_{-0.014}$	$15.29^{+0.10}_{-0.10}$
O I	$-2.164^{+0.100}_{-0.106}$	$14.86^{+0.01}_{-0.01}$
Si II	$-1.458^{+0.073}_{-0.077}$	$13.96^{+0.04}_{-0.04}$
P II	$-1.584^{+0.102}_{-0.109}$	$12.06^{+0.01}_{-0.01}$
Ar I	$-2.436^{+0.104}_{-0.110}$	$12.32^{+0.01}_{-0.01}$
Fe II	$-1.991^{+0.098}_{-0.103}$	$13.60^{+0.02}_{-0.01}$

<sup>a</sup> Radially averaged ratio of the ion number to the total number of the element.

<sup>b</sup> Column density in  $\text{cm}^{-2}$ .

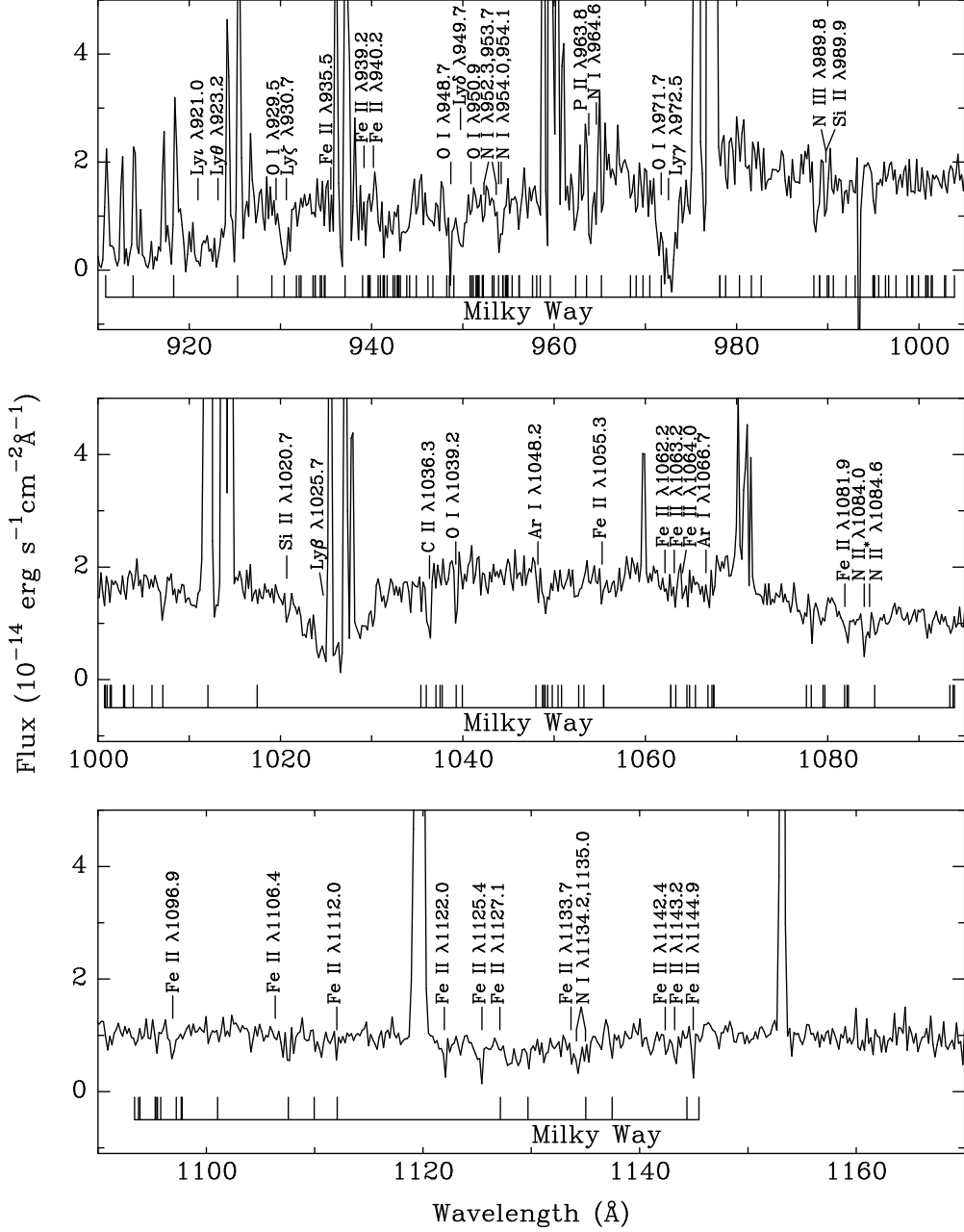


Fig. 1.— *FUSE* spectrum in the rest frame of SBS 0335–052 (shifted by  $4050 \text{ km s}^{-1}$ ). Here the data have been rebinned to a resolution of  $0.2 \text{ Å}$ . Prominent interstellar absorption lines are indicated. The lines arising in SBS 0335–052 are marked on top and those in the Milky Way at bottom. In addition to the  $\text{H}\alpha$  Lyman series in SBS 0335–052, there are also strong interstellar absorption lines from  $\text{C II}$ ,  $\text{N I}$ ,  $\text{N II}$ ,  $\text{O I}$ ,  $\text{Si II}$  and  $\text{Fe II}$ .

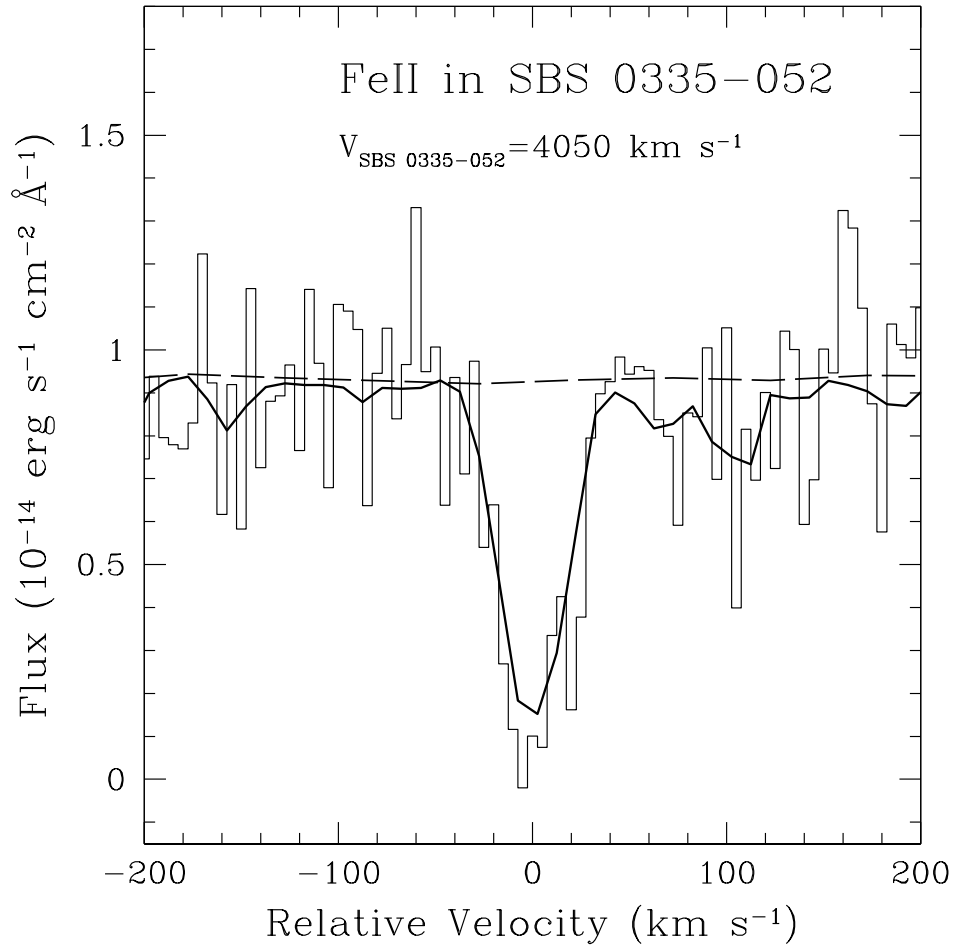


Fig. 2.— Co-added profile of the Fe II absorption line in SBS 0335–052. The profile and adjacent continua have been obtained by an error-weighted co-addition of 9 different Fe II lines at wavelengths  $\lambda_0 = 1055 \text{ \AA}$ ,  $1063 \text{ \AA}$ ,  $1064 \text{ \AA}$ ,  $1082 \text{ \AA}$ ,  $1097 \text{ \AA}$ ,  $1122 \text{ \AA}$ ,  $1125 \text{ \AA}$ ,  $1143 \text{ \AA}$  and  $1145 \text{ \AA}$ . The profile fits to individual lines have also been co-added, and the result is shown by a thick line. The dashed line shows the addition of the corresponding continua. Other lines can also be seen such as a  $\text{H}_2$  ( $J=1$ ) line and a Fe II line from the Milky Way at  $\sim 110 \text{ km s}^{-1}$ .

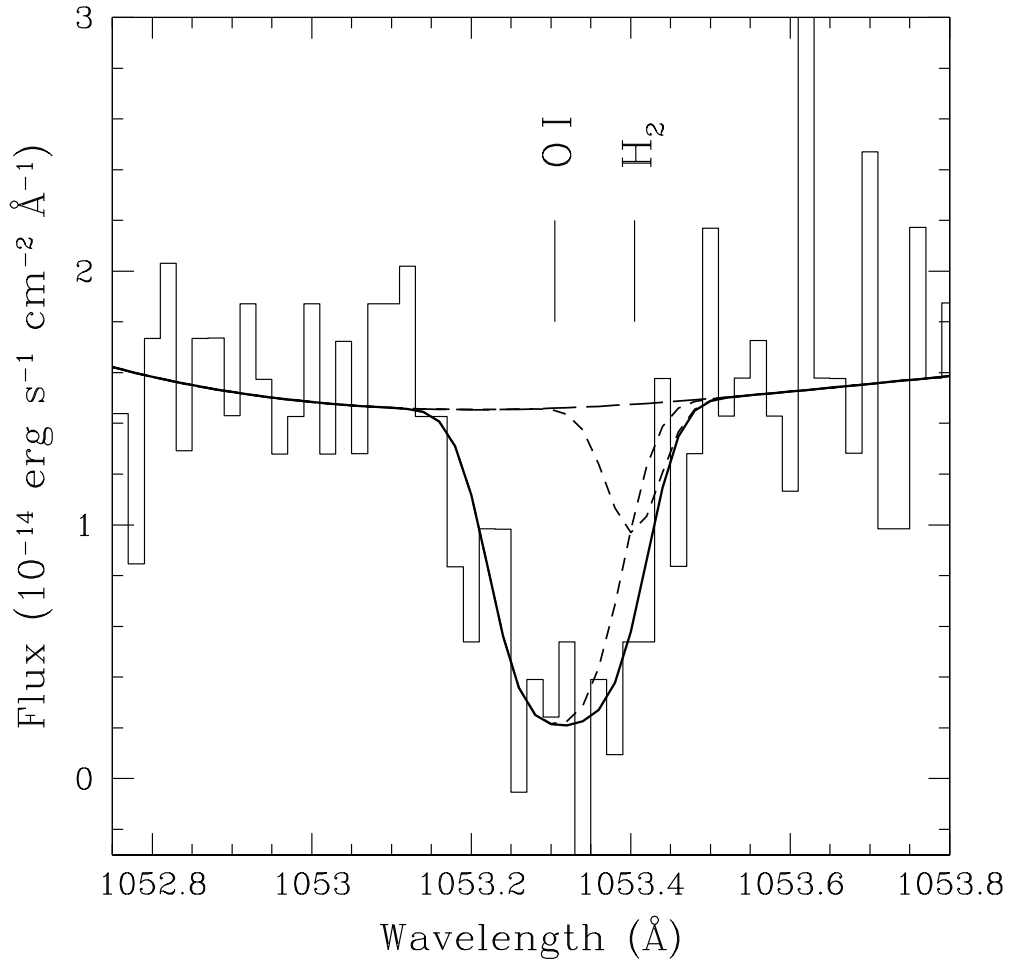


Fig. 3.— Profile of the O I  $\lambda$ 1039Å absorption line in the LiF1a channel. The fit is shown by small dashes while the continuum is shown by long dashes. The other absorption line at  $\lambda \sim 1053.4$  Å is due to Galactic H<sub>2</sub>. Its fit is also shown by small dashes. The sum of the two profiles is shown by the thick solid line which fits well the data (histogram).

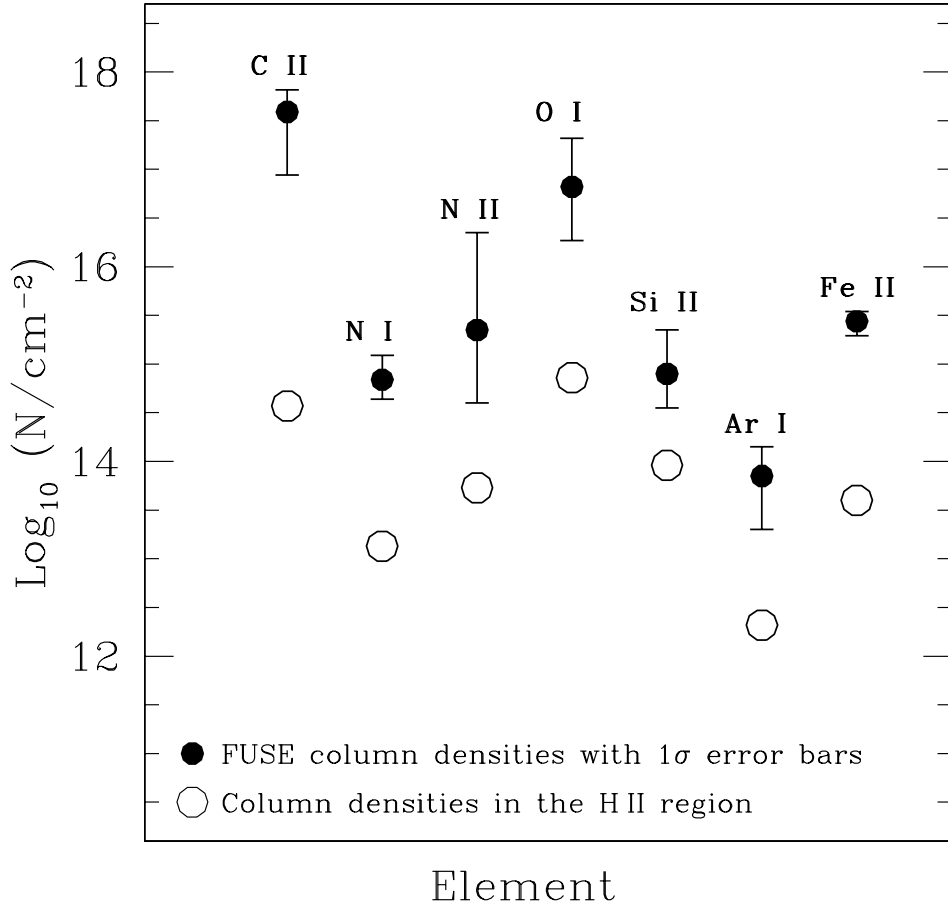


Fig. 4.— Heavy element column densities in the H I and H II gas of SBS 0335–052. The filled circles show the column densities derived from the *FUSE* data. The open circles show the column densities in the H II region as calculated from CLOUDY modeling of the optical emission lines. The column densities in the H I cloud follow the same pattern as the ones in the H II gas, although they are larger by 1-2 orders of magnitude. While this pattern reflects the cosmic abundances of the considered species, the fact that we recover this pattern shows the consistency of the measured column densities in the H I gas although they have been derived from low S/N data. The lower column densities in the ionized gas show that the absorption lines in the *FUSE* spectra arise in the neutral interstellar gas.

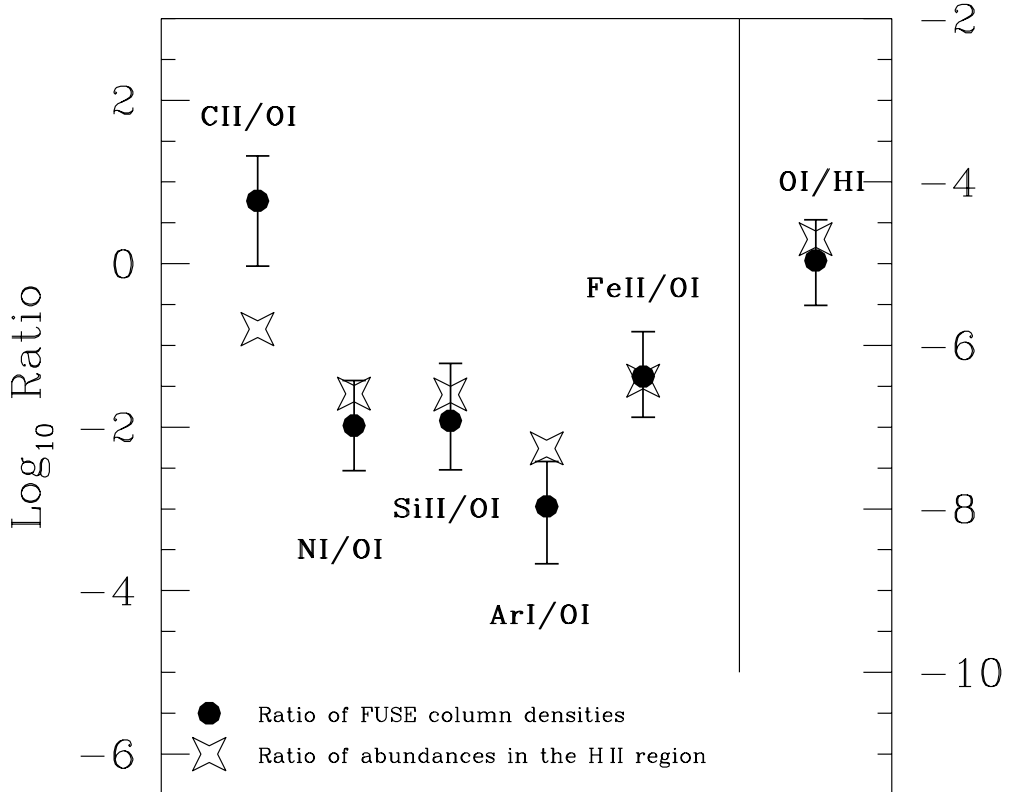


Fig. 5.— Relative ratios of *FUSE* column densities (filled circles) in the H I gas compared to the corresponding abundance ratios in the H II gas (stars) in SBS 0335–052. For each *FUSE* column density, the ionization state shown is the main one in the H I region and the ionization correction factors are very near unity. For the H II region, total element abundances including all ionization states are plotted. From left to right are the C/O, N/O, Si/O, Ar/O, Fe/O and O/H ratios. The right ordinate is for the O/H ratio, while the left ordinate is for all other abundance ratios. Note in particular that the O/H ratios in the H I and H II regions are very similar.